Journal of Engineering Mathematics **36:** 311–326, 1999.

Analysis of flux flow and the formation of oscillation marks in the continuous caster

JAMES M. HILL[1], YONG HONG WU[2] and BENCHAWAN WIWATANAPATAPHEE[2]
[1]*Department of Mathematics, The University of Wollongong, Wollongong, NSW 2500, Australia*
[2]*School of Mathematics and Statistics, Curtin University of Technology, WA 6845, Australia*

Received 8 January 1996; accepted in revised form 2 February 1999

Abstract. In the industrial process of continuous steel casting, flux added at the top of the casting mould melts and forms a lubricating layer in the gap between the steel and the oscillating mould walls. The flow of flux in the gap plays an essential role in smoothing the casting operation. The aim of the present work is to better understand the mechanics of flux flow, with an emphasis on such problems as how the flux actually moves down the mould, the physical parameters governing the consumption rate of the flux and the geometry of the lubricating layer. The problem considered is a coupled problem of liquid flow and multi-phase heat transfer. In the first part of the paper, the formation of the lubricating layer is analysed and a set of equations to describe the flux flow is derived. Then, based on an analysis of the heat transfer from the molten steel through the lubricating layer to the mould wall, a system of equations correlating the temperature field in the steel and flux with the geometry of the lubricating layer is derived. Subsequently, the equations for the flux flow are coupled with those arising from heat-transfer analysis and then a numerical scheme for the calculation of the consumption rate of flux, the geometry of the lubricating layer and the solidification surface of the steel is presented.

Key words: continuous steel casting, oscillation marks, lubrication theory, heat transfer, flux flows.

1. Introduction

In the industrial process of continuous steel casting, molten steel is poured continuously into a water-cooled mould, where intense cooling causes a thin solidified steel shell to form around the edges of the steel, leaving a large molten core inside the shell. The steel shell is then withdrawn from the bottom of the mould under support from closely spaced rolls. Figure 1 shows the essential features of the process. To facilitate this process and to prevent the molten steel from sticking to the mould wall, the mould wall oscillates vertically and mould powder is added at the top of the mould. The mould powder, being lighter than steel, melts and forms a liquid pool on the steel surface which is then drawn down between the mould wall and the steel providing lubrication, as a result of the oscillation. It is generally recognized that mould oscillation also causes small imperfections (notches) on the surface of the steel (see for example [1] and [2]). Thus, flux flow occurs between the mould wall and the casting surface which has regularly spaced notches. In order to optimize the process, a proper understanding of the flux flow is important, which can only be achieved with a proper analysis of the oscillation marks.

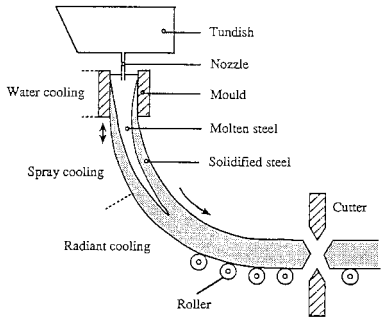

Figure 1. The continuous casting process.

Much of the physics of the casting process is understood (see for example [3–5] and various mathematical models have been developed to analyse the flux flow and evaluate the consumption rate of flux. The models due to Bland [6] and Fowkes and Woods [7], although promising, are incomplete and further work is still required. In the Bland [6] model, an important variable $h_0(t^*)$, which is the thickness of the flux layer at the top of the mould, needs to be prescribed and is determined by a process of trial and error. Accordingly, the application of this model is limited and the necessity to guess $h_0(t^*)$ is unrealistic. Although the Fowkes-and-Woods model [7] overcomes this shortcoming, in that it leads to a unique determination of $h_0(t^*)$, the coupling of the flux flow with the temperature field is omitted altogether. In addition, in both models, the presence of oscillation notches on the steel surface is not taken into account. Incorporating these notches we are led to an entirely different equation for the determination of the thickness of the flux channel and, consequently, the consumption rate of flux and this is the purpose of the present paper.

Here we present a model which takes into account the formation of oscillation notches on the steel surface and which couples the flux flow with the heat-transfer problem, so that the consumption rate of flux and the thickness of the flux flow channel can be evaluated accurately. The formation of oscillation marks is also considered by King *et al.* [8]. These authors treat the solidifying steel as a temperature-dependent viscous beam which is bent by the high pressures generated in the liquid flux. An initial analysis of their model is made, without a detailed numerical treatment. Our formulation is similar to that of King *et al.* [8], except that our analysis is based on a temperature-dependent viscosity, in which we couple the temperature distribution with the flux flow, and for which we present a full numerical solution in the presence of oscillation.

In the following section, we propose a possible mechanism to explain the formation of oscillation marks and, accordingly, we deduce Equation (2.2) relating the thickness $h(z^*, t^*)$ of flux flow channel at any depth with the thickness $h_0(t^*)$ at the solidification point of steel. In the section thereafter we establish equations relating the flux flow rate with the thickness of the flow channel for both the upper and lower parts separated by the solidification point of steel. Based on mass conservation, we derive in Section 4 the cubic Equation (4.3) for the determination of $h_0(t^*)$, obtained by matching the equations for the flow rates in the upper and lower zones. The resulting equation for $h_0(t^*)$ is highly dependent on the temperature in the flux. The heat-transfer analysis is presented in Section 5. In Section 6 of the paper we briefly describe an iterative scheme for the solution of the coupled mould oscillation-flux flow-heat-transfer problem for the case of neglecting the latent heat of the flux and numerical results are presented in the final section of the paper.

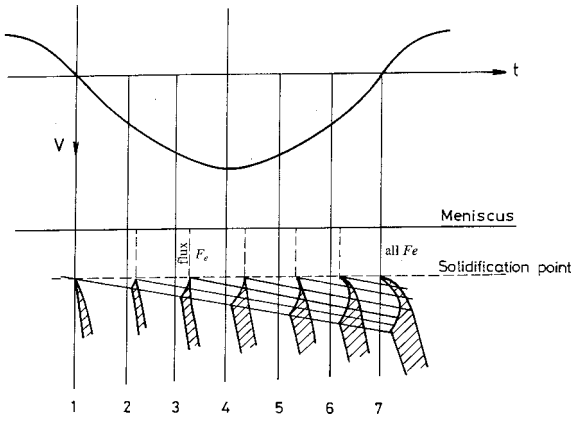

Figure 2. Schematic diagram showing the formation of oscillation marks.

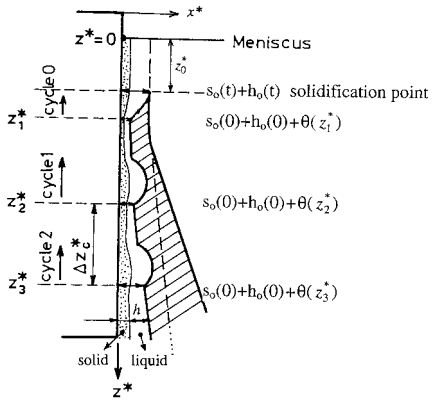

Figure 3. Schematic diagram showing the geometry of the flux channel.

2. The geometric form of the flux flow channel

Below the solidification point of steel, flux flows in the gap between the mould wall and the surface of the casting steel. Thus, the geometry of the flow channel is essentially determined by the surface contour of the casting. Since it has been observed in practice that the finished steel surface has oscillation marks in the form of regularly spaced notches, several possible mechanisms have been proposed to explain the formation of these notches (see for example [2]). In this section we deduce a formula to describe the thickness $h(z^*, t^*)$ of the flow channel at any depth z^* in terms of the thickness at the solidification point. We suppose that the solidified steel shell is covered by molten steel without a rigid solid skin on the top surface and that the solidified steel shell is withdrawn downwards with constant casting speed U. Under these assumptions, the formation of oscillation marks is shown schematically in Figure 2. We remark here that in the present model the steel solidification point is considered to be time dependent and for simplicity this time-dependent nature is not shown in the schematic diagram. The determination of the solidification point is based on the temperature field computed from thermal analysis which will be detailed in Sections 5 and 6. We also remark that, as the profile of the flux in the upper zone above the steel solidification point is not needed in the calculation of oscillation marks, the present work will not concern determination of the flux profile in the upper zone and thus the geometry of the flux layer shown in Figure 2 is a sketch only.

During the downward stroke of the mould wall, flux is dragged into the lubrication zone and the molten steel is pushed away from the mould wall by the positive pressure generated in the flux and thus a flow channel is formed. On increasing the downward speed (stages 1–4), the thickness of the channel increases. However, with decreasing downward speed (stages 4–7), the thickness of the channel decreases. During the upstroke of the mould wall, one may expect that flux will be carried upwards. However, suction forces within the liquid flux layer reduce the width of the liquid flux layer to zero and the molten steel entirely fills the upper part of the mould and thus prevents a significant amount of flux being dragged upwards. The molten steel above the solidification point thus acts as the valve of a pump, allowing the liquid flux moving downward but prevent it moving upward. This pumping mechanism has been analysed in detail by Fowke and Wood [7] and thus we will not repeat the details here. According to

this analysis, each oscillation cycle produces one notch on the steel surface. Thus regularly spaced notches appear on the steel surface and the geometry of the flux channel is as shown in Figure 3. The pitch of oscillation marks is equal to the withdraw speed of the solid steel multiplied by the period of one oscillation cycle. If we denote the period of one oscillation cycle as t_c^* and the pitch of the notches as Δz^*, then we have

$$t_c^* = \frac{2\pi}{\omega}, \qquad \Delta z^* = \frac{2\pi}{\omega} U, \tag{2.1}$$

where ω and U denote the angular frequency of oscillation and the casting speed, respectively.

Further, we note that, as the casting moves downwards, the solidified steel shell increases in thickness and cools which consequently causes the casting to contract. The deformation of the solidified steel shell is due to both thermal contraction of steel and the difference of liquid pressures inside and outside the shell. An exact analysis requires solving a three-dimensional thermal viscoelastic (or thermal viscoelastic-plastic) problem which would be extremely difficult. To facilitate the analysis, while retaining the fundamental physics of the problem, we adopt the strategy of keeping the model for the solidified layer as simple as possible. Above the solidification point, the steel is very soft and thus the steel-flux interface is allowed to move toward and away from the mould wall as the lubrication pressure varies. Below the solidification point, the solidified steel shell is assumed to be very stiff, that is, the deformation due to the lubrication pressure is assumed to be negligible. The omission of the deformation due to the lubrication pressure, although affecting the accuracy of the estimation of total deformation, is expected to still retain the fundamental physics regarding the formation of oscillation marks. Because firstly, for a particular horizontal cross-section, the pressure-induced deformation of the section, when it is below the solidification point, is expected to be much smaller than that when the section is above the solidification point. Secondly, the purpose of the present work is to analyse the formation of oscillation marks and for this purpose only the relative deformation at different locations is essential. As every horizontal cross-section of the steel cast goes through the same path in the casting process, the total pressure-induced deformation, accumulated during the period when the section moves from the top to the bottom of the mould, is expected to be approximately the same for different cross-sections. Thus, the pressure-induced deformation on the lower part of the solidification point will not significantly affect the relative deformation field. It is also noted that the stiff-beam assumption for the solidified steel shell has also been used by other researchers (see for example [6] and [8]). Hence, the thickness of the flux layer at any cross-section with depth z^* is equal to the thickness of the layer when it lies at $z^* = z_0^*$ plus the thermal contraction due to cooling. If we choose a time coordinate t^*, with $t^* = 0$ representing the beginning of the mould wall downstroke, then at an instant t^* of the ith oscillation cycle, the cross-section which lay at solidification point $z^* = z_0^*$ at $t^* = 0$ of cycle 0 will be in the position $z_i^* = z_0^* + Ut^* + 2\pi iU/\omega$, as shown in Figure 3. Thus, as a typical instant of time t^*, a cross section at z^* lying between z_i^* and z_{i+1}^* was at the solidification point (starting to solidify) at time $t_0^* = t^* - (z^* - z_0^* - i\Delta z^*)/U$. Thus, we have the relation

$$\begin{aligned} &s(z^*, t^*) + h(z^*, t^*) \\ &\quad = s_0\left[\frac{t^* - (z^* - z_0^* - i\Delta z^*)}{U}\right] + h_0\left[\frac{t^* - (z^* - z_0^* - i\Delta z^*)}{U}\right] + \theta(z^*, t^*), \end{aligned} \tag{2.2}$$

where $\theta(z^*, t^*)$ represents the thermal contraction due to cooling during the period when the cross section travels from z_0^* to z^*. Assuming that each horizontal section of the mould

contracts independently of other sections and that the amount of the contraction $\theta(z^*, t^*)$ is the same as that which would occur if the whole section was reduced in temperature from a uniform value of the melting point S_M^* to the uniform value of the average temperature of the steel $(S_m^* + T_0^*)/2$ where T_0^* denotes $T^*(s + h, z^*, t^*)$, we have

$$\theta(z^*, t^*) = \lambda(S_m^* - T_0^*), \tag{2.3}$$

where $\lambda = \varepsilon M/2$ and ε and M are the coefficient of linear thermal expansion of steel and the distance of the mould surface to the central line, respectively.

3. Transport of flux down the mould

In the pumping-action model of flux flow down the mould originally proposed by Fowkes and Woods [7], the flow zone is divided into an upper zone and lower zone separated by the solidification point of steel and the dynamics in these zones is analysed separately. By matching the equations for the flow rate in the upper and lower zones at the transition point, we obtain a quadratic equation for the determination of the thickness of the flux channel in the upper zone and consequently the consumption rate of flux. In this section, we follow the Fowkes-and-Woods pumping-action model [7], but in addition we take into account the presence of oscillation notches in the steel surface and also discard Fowkes-and-Woods' assumption of independence on the volume flow rate with depth z^*.

For the transport of flux in the upper part, Fowkes and Woods [7] assume that the flow of liquid flux is governed by the lubrication equation

$$\frac{\partial P}{\partial z^*} = \frac{\partial}{\partial x^*}\left(\mu \frac{\partial u}{\partial x^*}\right) + \rho_f g^*, \tag{3.1}$$

where $P(z^*)$ is the pressure assumed independent of x^*, μ is the temperature dependent viscosity, ρ_f is the flux density, g^* is the acceleration due to gravity and $u(x^*, z^*)$ denotes the flux velocity in the z^* direction. Equation (3.1) is subject to the two boundary conditions that the surface of the flux layer adjacent to the mould wall moves with the mould wall at the same speed V and that the other boundary with the molten steel is sufficiently smooth to allow slipping. Based on these assumptions, the volume flow rate of liquid flux is related to h by the equation

$$Q_l = Vh - \Delta\rho g^* \int_0^h \frac{(h-\zeta)^2}{\mu(\zeta + s, z^*)}\,\mathrm{d}\zeta, \quad 0 \leqslant z^* \leqslant z_0^*, \tag{3.2}$$

where s and h denote the thickness of the solid and liquid flux layer respectively. An alternative expression for Q_l is given by Fowkes *et al.* [9] in which the flux/steel interface is assumed to move downward with casting speed U, instead of imposing a slip condition. However, since in the casting process, circulation of molten steel occurs in the top part of the mould and the molten steel near the wall at the top part moves upwards due to the thermal buoyancy force, we therefore adopt the Fowkes-and-Woods' assumption for the present work.

Although Equation (3.2) determines neither the flow rate nor the thickness of the lubricating layer, it indicates that there exists an upper limit for the volume flow rate. For example, in

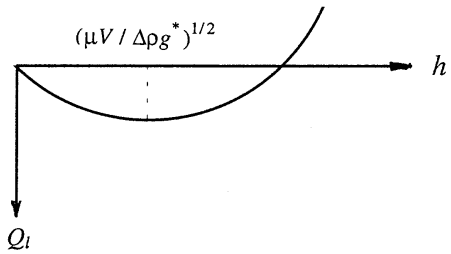

Figure 4. Schematic diagram showing the relation between Q_l and h.

the case when μ is a constant, the $Q_l - h$ relation is shown in Figure 4 and the maximum flow rate occurs at $h = (\mu V/\Delta\rho g^*)^{1/2}$ and has magnitude

$$Q_{l_{\max}} = \frac{2}{3}\left(\frac{\mu}{\Delta\rho g^*}\right)^{1/2} V^{3/2}. \tag{3.3}$$

Thus, Equation (3.3) can be used as an upper bound for the volume flow rate. Further, although the profiles of both the solid flux and liquid flux in the upper part of the solidification point are not required in the calculation of oscillation marks, as can be seen in later sections, we remark that equations for $h(z^*, t^*)$ and $s(z^*, t^*)$ can be derived from the principles of heat and mass conservation, see for example [8] for the partial differential equation which the $h(z^*, t^*)$ must satisfy.

In order to construct a defining equation for the thickness of the flux channel and the consumption rate of flux, we now consider the flow of flux in the lower zone. Based on the standard lubrication theory, we assume that

(a) the flux behaves as a Newtonian fluid,
(b) inertial force can be neglected because the fluid velocity is low and the flux viscosity is high,
(c) flux velocities in the transverse direction (normal to the mould wall) are negligible compared with those downwards.

Under these assumptions, the fluid flow in the flux channel is governed by the equation of motion (3.1) and the mass continuity equation

$$\frac{\partial(Q_s + Q_l)}{\partial z^*} + \frac{\partial(h+s)}{\partial t^*} = \frac{\partial}{\partial z^*}\left(Vs + \int_0^h u(s+\zeta, t^*)\,\mathrm{d}\zeta\right) + \frac{\partial(h+s)}{\partial t^*} = 0, \tag{3.4}$$

where Q_s and Q_l denote the flow rates of solid and liquid fluxes respectively, and the solid flux adjacent to the mould wall has been assumed to move with the mould wall at the same speed V. In addition, since the flux/steel interface moves downwards with casting speed U, we have from (2.2), by partial differentiation, the additional equation

$$\frac{\partial(h+s)}{\partial t^*} + U\frac{\partial(h+s)}{\partial z^*} = \frac{\partial\theta}{\partial t^*} + U\frac{\partial\theta}{\partial z^*}, \tag{3.5}$$

which is solved together with the pressure boundary conditions

$$P(z_0^*) = \rho g^* z_0^*, \qquad P(L) = 0, \tag{3.6}$$

and the boundary conditions for velocity on the solid flux/liquid flux and the liquid flux/steel interfaces,

$$u(s, t^*) = V(t^*), \qquad u(s + h, t^*) = U, \tag{3.7}$$

where here a noslip condition has been assumed for the interfaces and liquid is assumed to remain in the flux channel, *i.e.* $L > 0$. We remark that in the Fowkes-and-Woods model [7], the presence of oscillation marks is neglected and thus the cooling surface is approximated by the doted line shown in Figure 3. In addition, instead of Equations (3.4) and (3.5), it is assumed that $Q_l + Q_s = Q(t^*)$.

When the casting process is in smooth operation, the variation of temperature and consequently the thermal contraction θ with time is expected to be much smaller than the variation along the casting direction z^*. Thus $\partial\theta/\partial t^*$ is neglected to simplify the analysis, while still retaining the fundamental feature of the problem. We also note that in an early model [8], both $\partial\theta/\partial t^*$ and $\partial\theta/\partial z^*$ are neglected. Hence, from Equations (3.4) and (3.5), we may deduce

$$Vs + \int_0^h u(\zeta + s, t^*)\,\mathrm{d}\zeta - U(h + s - \theta) = Q_R(t^*). \tag{3.8}$$

While from Equations (3.1) and (3.7) we obtain (see Bland [6] and Fowkes and Woods [7] for similar calculations)

$$Q_l = \int_s^{s+h} u(x, t^*)\,\mathrm{d}x = U[h - f(h)] + Vf(h) - g(h)\left(\frac{\partial P}{\partial z^*} - \rho_f g^*\right), \tag{3.9}$$

where

$$\begin{aligned} f(h) &= \int_0^h \frac{\zeta}{\mu(\zeta + s, z^*)}\,\mathrm{d}\zeta \left(\int_0^h \frac{\mathrm{d}\zeta}{\mu(\zeta + s, z^*)}\right)^{-1}, \\ g(h) &= \int_0^h \frac{\zeta}{\mu(\zeta + s, z^*)}\,\mathrm{d}\zeta - \left(\int_0^h \frac{\zeta}{\mu(\zeta + s, z^*)}\,\mathrm{d}\zeta\right)^2 \left(\int_0^h \frac{\mathrm{d}\zeta}{\mu(\zeta + s, z^*)}\right)^{-1}. \end{aligned} \tag{3.10}$$

On substitution of (3.9) in (3.8) and using (3.6), we obtain the lower zone relation between Q_l and h,

$$\begin{aligned} Q_l &= Q_R + U(h + s - \theta) - Vs \\ &= \frac{1}{\int_{z_0^*}^L \frac{\mathrm{d}z}{g(h)}} \left\{ \Delta\rho g^* z_0^* + \rho_f g^* L + (V - U) \int_{z_0^*}^L \frac{[s + f(h)]}{g(h)}\,\mathrm{d}z \right\} \\ &\quad + U(h + s - \theta) - Vs, \quad z_0^* < z^* < L, \end{aligned} \tag{3.11}$$

Just as for Equation (3.2) for the flow of flux in the upper part, Equation (3.11) itself determines neither the flow rate nor the thickness of flux layer. However, by matching (3.2) with (3.11) at $z^* = z_0^*$, we can deduce a useful equation which we detail in the following section.

4. Matching upper and lower zone models for flux conservation

From mass conservation, the flow rate of flux evaluated by Equation (3.11) for the lower zone should be equal to that evaluated by Equation (3.2) for the upper part at their transition point $z^* = z_0^*$. Thus, by equating the right-hand side of Equation (3.2) with the right-hand side of Equation (3.11) at $z^* = z_0^*$ and noting that $\theta(z_0^*, t^*) = 0$, we obtain

$$\Delta\rho g^* \int_0^h \frac{(h_0 - \zeta)^2}{\mu(\zeta + s_0, z^*)}\,\mathrm{d}\zeta \;=\; (V - U)\left\{ s_0 + h_0 - \frac{\int_{z_0^*}^{L} \frac{[s+f(h)]}{g(h)}\,\mathrm{d}z}{\int_{z_0^*}^{L} \frac{\mathrm{d}z}{g(h)}} \right\}$$

$$- \frac{\Delta\rho g^* z_0^* + \rho_f g^* L}{\int_{z_0^*}^{L} \frac{\mathrm{d}z}{g(h)}} - U \frac{\int_{z_0^*}^{L} \frac{\theta}{g(h)}\,\mathrm{d}z}{\int_{z_0^*}^{L} \frac{\mathrm{d}z}{g(h)}}. \tag{4.1}$$

To obtain a simpler form of this equation, we consider two special cases. For the first case, we assume that the viscosity coefficient μ is a constant, and thus form (3.10) we have

$$f(h) = \frac{h}{2}, \qquad g(h) = \frac{h^3}{12\mu}, \tag{4.2}$$

and substitution of (4.2) in (4.1) gives rise to

$$\frac{\Delta\rho g^*}{3\mu} h_0^3 \;=\; (V - U)\left\{ h_0 + s_0 - \frac{\int_{z_0^*}^{L} \frac{2s+h}{h^3}\,\mathrm{d}z}{2\int_{z_0^*}^{L} \frac{1}{h^3}\,\mathrm{d}z} \right\}$$

$$- \frac{\Delta\rho g^* z_0^* + \rho_f g^* L}{12\mu \int_{z_0^*}^{L} \frac{1}{h^3}\,\mathrm{d}z} - U \frac{\int_{z_0^*}^{L} \frac{\theta}{h^3}\,\mathrm{d}z}{\int_{z_0^*}^{L} \frac{1}{h^3}\,\mathrm{d}z}. \tag{4.3}$$

For the second case, following Bland [6] we assume that the variation of viscosity with temperature obeys the Reynolds' law, that is

$$\mu(x^*, z^*) = A\,\mathrm{e}^{-BT^*(x^*, z^*, t^*)}, \tag{4.4}$$

where A and B denote constants.

As the liquid flux layer is very thin, we assume that at any cross-section z^*, the temperature T^* varies linearly with x^* across the liquid flux layer with $T^* = T_0^*(z^*, t^*)$ on $x^* = s + h$ and $T^* = T_m^*$ on $x^* = s$, that is

$$T^*(x^*, z^*, t^*) = T_m^* + \frac{T_0^* - T_m^*}{h(z^*, t^*)}(x^* - s) \quad (s < x^* \leqslant s + h), \tag{4.5}$$

we have from (4.4)

$$\mu(x^*, z^*) = A\,\mathrm{e}^{-BT_m^*} \exp\left(-\frac{T_0^*(z^*, t^*) - T_m^*}{h(z^*, t^*)} B(x^* - s) \right), \tag{4.6}$$

so that from (3.10), we can deduce

$$\left.\begin{aligned} f(h) &= \frac{1}{\eta}\left(\frac{\eta\,\mathrm{e}^{\eta}}{\mathrm{e}^{\eta}}-1\right)h(z^*,t^*) = F(z^*,t^*)h(z^*,t^*) \\ g(h) &= \frac{\mathrm{e}^{BT_m^*}}{A\eta^3}\{\mathrm{e}^{\eta}-1-\eta^2[1-\mathrm{e}^{-\eta}]^{-1}\}h^3(z^*,t^*) = G(z^*,t^*)h^3(z^*,t^*) \end{aligned}\right\}, \tag{4.7}$$

where $F(z^*,t^*)$ and $G(z^*,t^*)$ are as defined above and

$$\eta(z^*,t^*) = B[T_0^*(z^*,t^*) - T_m^*]. \tag{4.8}$$

Substitution of (4.7) in (4.1) yields

$$\Delta\rho g^*\Theta(\eta_0)h_0^3 \;=\; (V-U)\left\{s_0 + h_0\frac{\int_{z_0^*}^{L}\frac{s+Fh}{Gh^3}\,\mathrm{d}z}{\int_{z_0^*}^{L}\frac{\mathrm{d}z}{Gh^3}}\right\}$$

$$-\frac{\Delta\rho g^* z_0^* + \rho_f g^* L}{\int_{z_0^*}^{L}\frac{\mathrm{d}z}{Gh^3}} - U\frac{\int_{z_0^*}^{L}\frac{\theta}{Gh^3}\,\mathrm{d}z}{\int_{z_0^*}^{L}\frac{1}{Gh^3}\,\mathrm{d}z}, \tag{4.9}$$

where

$$\Theta(\eta_0) = A^{-1}\,\mathrm{e}^{BT_m}\eta_0^{-3}(2\,\mathrm{e}^{\eta_0} - \eta_0^2 - 2\eta_0 - 2), \quad \eta_0 = \eta(z_0^*,t^*). \tag{4.10}$$

It is apparent that neither of (4.3) or (4.9) can be solved directly since the determination $s(z^*,t^*)$, $h(z^*,t^*)$ and $\theta(z^*,t^*)$ requires the solution of the temperature T_0^* on the steel casting surface. The necessary heat transfer analysis is carried out in the following section.

5. Governing equations arising from thermal analysis

In the continuous casting process, heat flows from the liquid steel across the layers of solid steel casting, liquid flux and solid flux, into the surrounding mould from which the heat is removed by the cooling water. The aim of the heat-transfer analysis is to construct additional equations relating the thermal variables such as temperature with the flow variables such as μ, h_0, s_0 and θ, so that on combining these relations with the defining equations described in Section 4, a closed system of equations can be formed for the determination of both the temperature field and the flux flow in the flux channel.

Since the flux layer is very thin, it is reasonable to approximate the temperature profile by a linear function across the thickness. Thus, on denoting the temperatures on the mould wall, solid flux surface adjacent to the mould, solid/liquid flux interface and flux/steel interface as T_w^*, T_μ^*, T_m^* and T_0^*, respectively, and considering the heat balance on the mould wall $x^* = 0$ and solid/liquid flux interface $x^* = s$, we have for $s \neq 0$ and $h \neq 0$,

$$Q = k_s\frac{T_m^* - T_\mu^*}{s} = \frac{T_\mu^* - T_w^*}{R} = m(T_w^* - T_\infty^*), \tag{5.1}$$

and

$$\left.\begin{aligned} &\rho_f l_f\left(\frac{\partial s}{\partial t^*} + V\frac{\partial s}{\partial z^*}\right) = k_s\frac{T_m^* - T_\mu^*}{s} - k_l\frac{T_0^* - T_m^*}{h}, \\ &s(z_0^*,t^*) = s_0(t^*), \qquad s(z^*,0) = \widehat{s}(z^*), \end{aligned}\right. \tag{5.2}$$

where $\widehat{s}(z^*)$ denotes thickness of solid flux layer at $t^* = 0$ and k_s and k_l denote thermal conductivities of solid and liquid fluxes, respectively. The determination of $\widehat{s}(z^*)$ requires an iterative process starting with an initial guess. For $s = h = 0$ we have

$$T_w^* = \frac{S_m^* + RT_\infty^*}{1 + mR}. \tag{5.3}$$

In the region of steel we may deduce, in a similar manner to that detailed in Hill and Wu [10], the governing equations which comprise the heat-conduction equation

$$\rho c \left(\frac{\partial T^*}{\partial t^*} + U \frac{\partial T^*}{\partial z^*} \right) = k \frac{\partial^2 T^*}{\partial x^{*^2}}, \tag{5.4}$$

the solid/liquid interface conditions

$$\begin{aligned} &T^*(s + h + X^*, z^*, t^*) = S_m^*, \\ &k \frac{\partial T^*}{\partial x^*}(s + h + X^*, z^*, t^*) = \rho l \left(U \frac{\partial X^*}{\partial z^*} + \frac{\partial X^*}{\partial t^*} \right), \end{aligned} \tag{5.5}$$

the boundary conditions on the casting steel surface and the symmetric plane

$$k \frac{\partial T^*}{\partial x^*}(s + h, z^*, t^*) = k_l \frac{T_0^* - T_m^*}{h}, \qquad \frac{\partial T^*}{\partial x^*}(M, z^*, t^*) = 0, \tag{5.6}$$

and the initial conditions

$$T^*(x^*, z_0^*, t^*) = S_m^*, \qquad \frac{\partial T^*}{\partial t^*}(x^*, z^*, 0) = q_0(x^*, z^*), \qquad X^*(z_0^*, t^*) = 0, \tag{5.7}$$

where q_0 is the time rate of T^* at $t^* = 0$ and can be determined through an iterative process starting with an initial guess. We remark here that in the molten-steel region, transfer of heat is due to both conduction and convection in the directions of x^* and z^* and thus the exact heat-transfer equation will be much more complicated than Equation (5.4). However, by considering the characteristics of heat transfer in continuous casters and the fact that the temperature variation in molten steel is very small (usually the temperature of molten steel from the nozzle is only a few degree higher than the solidification temperature), we can make two simplifications without significantly affecting the accuracy of results. Firstly, as cooling water is in the channels of the mould wall, the temperature gradient in the x^*-direction is much larger than that in the z^*-direction, namely $\partial T^*/\partial x^* \gg \partial T^*/\partial z^*$. Hence, the z^*-component of the heat-flow vector (the z^*-conduction term) is neglected as it is negligible compared to that in the x^*-direction. In other words, the term $\partial^2 T^*/\partial z^{*2}$ can be omitted compared to $\partial^2 T^*/\partial x^{*2}$. For a more detailed explanation, we refer readers to Bland [6] and Wu and Hill [5]. Secondly, we can consider the transfer of heat by convection in the molten-steel region using an effective thermal conductivity reported by Lait *et al*. [11] to be about seven times greater than the liquid thermal conductivity. These two simplifications will eventually lead to Equation (5.4) for the transfer of heat in the molten steel region.

Assumng that $h_0(t^*)$ and $s_0(t^*)$ are known, we observe that Equations (5.1)–(5.7), together with Equation (2.2), form a closed system which can be solved and the method for the solution is now discussed.

From (5.1) we can deduce that

$$T_\mu^* = \frac{k_s(1+mR)T_m^* + smT_\infty^*}{k_s(1+mR)+sm}, \qquad T_w^* = \frac{m(s+Rk_s)T_\infty^* + k_sT_m^*}{k_s(1+mR)+sm}, \tag{5.8}$$

and substitution of (5.8) and (2.2) in (5.2) yields

$$\rho_f l_f \left(\frac{\partial s}{\partial t^*} + V\frac{\partial s}{\partial z^*}\right) = \frac{mk_s(T_m^* - T_\infty^*)}{k_s(1+mR)+sm} - \frac{k_l(T_0^* - T_m^*)}{s_0 + h_0 + \theta - s}. \tag{5.9}$$

In order to simplify the notation, we now introduce the following unstarred variables defined by

$$\begin{aligned}
&x = \frac{x^*}{M}, \qquad X = \frac{X^*}{M}, \qquad z = \frac{k}{\rho c U M^2}z^*, \qquad t = \frac{k}{\rho c M^2}t^*, \\
&T(T^*) = \frac{k_l(S_m^* - T^*)}{k_s(T_m^* - T_\infty^*) + k_l(S_m^* - T_m^*)}, \qquad H(T) = \begin{cases} T+\alpha; & T>0 \\ [0,\alpha]; & T=0 \end{cases}, \\
&\alpha = \frac{lk_l}{c[k_s(T_m^* - T_\infty^*) + k_l(S_m^* - T_m^*)]},
\end{aligned} \tag{5.10}$$

and where the normalized (or nondimensional) enthalpy $H = 0$ represents the liquid state at the fusion point $T = 0$ while $H = \alpha$ corresponds to the solid state at the fusion point. In terms of the new variables the governing equations can be expressed as

$$\begin{aligned}
&\frac{\partial H}{\partial t} + \frac{\partial H}{\partial z} = \frac{\partial^2 T}{\partial x^2}, \\
&\frac{\partial T}{\partial x}(1,z,t) = 0, \qquad \frac{\partial T}{\partial x}(s+h,z,t) = \frac{Mk_l}{k}\frac{[T(s+h,z,t) - T_m]}{s_0 + h_0 + \theta - s}, \\
&H(x,z_0,t) = 0, \qquad \frac{\partial T}{\partial t}(x,z,0) = -\frac{\rho c^2 M^2 \alpha}{kl}q_0(x,z), \\
&\frac{\partial s}{\partial t} + W(t)\frac{\partial s}{\partial z} = \bar{F}[T(s+h,z,t), s], \\
&s(z_0,t) = s_0(t), \qquad s(z,t_0) = \widehat{s}(z),
\end{aligned} \tag{5.11}$$

where T_m denotes $T(T_m^*)$, H is defined by $(5.10)_6$ and $W(t)$ and $\bar{F}$ are, respectively, defined by

$$W(t) = \frac{V(t)}{U}, \qquad \bar{F}(T_0,s) = \frac{\rho l M^2}{\rho_j l_f k \alpha}\left\{\frac{mk_s(T_\infty - T_m)}{k_s(1+mR)+ms} + \frac{k_l(T_0 - T_m)}{s_0+h_0+\theta-s}\right\}. \tag{5.12}$$

If $s_0(t)$ and $h_0(t)$ are assumed known, then we can solve the system (5.11) using an iterative enthalpy scheme. However, since $s_0(t)$ and $h_0(t)$ are presently unknown functions which depend on the temperature field, a coupling of the system (5.11) with (4.3) or (4.9) is necessary in order to solve the problem. A numerical procedure leading to the solution of the coupled system is presented in the following sections.

6. Method of solution neglecting latent heat flux

In this section we detail the numerical procedure for the case in which the latent heat of flux is neglected. The purpose of neglecting latent heat is to simplify the computation. We believe that this omission may not significantly affect the accuracy, as the flux layer is very thin and thus the latent heat released by the flux layer is negligible compared to the total heat removed from the molten steel. Of course, a further study on the influence of the flux latent heat is certainly useful and that is why we retain the latent heat in the formulation of Section 5. Now on neglecting the latent heat in the flux, we obtain from Equations $(5.11)_{3,6}$

$$\frac{k}{M}\frac{\partial T}{\partial x}(s+h,z,t)=\frac{k_l(T_0-T_m)}{h}=\frac{mk_s(T_m-T_\infty)}{k_s(1+mR)+ms}, \tag{6.1}$$

where $T_0=T(s+h,z,t)$ and $h=s_0+h_0+\theta-s$. Further from (6.1) we can deduce that

$$s(z,t)=\frac{1}{\tau}h-k_s\left(R+\frac{1}{m}\right),\qquad h(z,t)=\frac{\tau}{1+\tau}\left\{\frac{1+\tau_0}{\tau_0}h_0+\lambda(S_m-T_0)\right\}, \tag{6.2}$$

where τ and τ_0 are defined by

$$\tau(z,t)=\frac{k_l(T_0(z,t)-T_m)}{k_s(T_m-T_\infty)},\quad \tau_0=\tau(z_0,t). \tag{6.3}$$

Thus, the surface boundary condition for the steel region $(5.11)_3$ can be simplified to give

$$T(s+h,z,t)-[\beta+\gamma T(s+h,z,t)]\frac{\partial T}{\partial x}(s+h,z,t)=1. \tag{6.4}$$

where $\beta(t)$ and γ are defined by

$$\begin{aligned}\beta&=\frac{k}{Mk_l}\left\{\frac{1+\tau_0}{\tau_0}h_0+(k_s-1)\left(R+\frac{1}{m}\right)\right\},\\ \gamma&=\frac{\lambda k}{Mk_l^2}\{k_s(T_m^*-T_\infty^*)+k_l(S_m^*-T_m^*)\}.\end{aligned} \tag{6.5}$$

Given a function $h_0(t)$, the temperature field $T(x,z,t)$ is completely defined by $(5.11)_{1,2,4,5}$ and (6.4) which can be solved by an enthalpy scheme similar to that detailed by Hill and Wu [10].

Since $h_0(t)$ as given by either (4.3) or (4.9) remains unknown and depends on the temperature field to be solved, coupling of the governing heat-transfer equations with (4.3) or (4.9) is necessary. Proceeding to describe the solution scheme, we first simplify Equation (4.3) using (6.2) to obtain

$$h_0^3+ph_0+q(h_0)=0, \tag{6.6}$$

where p and $q(h_0)$ are defined by

$$\begin{aligned}p&=-\frac{3\mu(V-U)}{\Delta\rho g^*}\frac{(1+\tau_0)}{\tau_0},\\ q(h_0)&=\frac{3\mu(V-U)}{\Delta\rho g^*}\left\{k_s\left(R+\frac{1}{m}\right)+\frac{\int_{z_0^*}^{L}\frac{2s+h}{h^3}\,\mathrm{d}z}{2\int_{z_0^*}^{L}\frac{1}{h^3}\,\mathrm{d}z}\right\}\\ &\quad+\frac{1}{4\Delta\rho}\frac{\Delta\rho z_0^*+\rho_f L}{\int_{z_0^*}^{L}\frac{1}{h^3}\,\mathrm{d}z}-\frac{3\mu U}{\Delta\rho g^*}\frac{\int_{z_0^*}^{L}\frac{\theta}{h^3}\,\mathrm{d}z}{\int_{z_0^*}^{L}\frac{1}{h^3}\,\mathrm{d}z},\end{aligned} \tag{6.7}$$

with s, h given by (6.2).

The iteration procedure for solving the temperature field and $h_0(t)$ is summarized as follows

(a) assign an initial value $h_0^0(t)$ to $h_0(t)$;
(b) calculate the temperature field $T^i(x^*, z^*, t^*)$ corresponding to $h_0^i(t)$ using the enthalpy method, then determine the location of the solidification point z_0^* from $T^i(x^*, z^*, t^*)$;
(c) evaluate h^i then p^i, q^i using (6.2) and (6.7) based on the computed temperature field T^i and h_0^i (the integrals involved are evaluated numerically using the composite trapezoidal rule);
(d) solve Equation (6.6) for h_0^{i+1};
(e) replace h_0^i by h_0^{i+1} then go back to step (b);
(f) the process repeated until successive calculations for $h_0(t)$ differ negligibly.

With above algorithm for solving the temperature field and $h_0(t)$, the procedure for calculating the geometry of the flux flow channel is as follows

(a) choose initial guesses for $\widehat{s}(z)$ and $q_0(x, z)$;
(b) determine the geometry of the flux channel by calculating $h_0(t_i)$ and updating $h(z, t_i)$ for $t_i = \Delta t, 2\Delta t, \ldots, n\Delta t$, where $n\Delta t$ is the time taken for the casting to move downwards from the solidification point to the exit of the mould;
(c) update $\widehat{s}(z)$ and $q_0(x, z)$ using the results obtained in (b) and then perform step (b) again. The process is repeated until convergence is achieved.

7. Numerical results and conclusions

In this section we illustrate the procedure of the previous section in the case when the latent heat of flux is neglected. Based on the model presented, a computer program has been developed for the calculation of flux flow rate and the prediction of oscillation marks on the steel surface. In the following we present the results obtained using the algorithm given in Section 6. Typical values for the geometrical and physical data were chosen as follows

Table 1. Numerical data.

$M = 0{\cdot}118\,\text{m}$	$k_l = 2{\cdot}25\,\text{W/m}\,^\circ\text{C}$	$g^* = 9{\cdot}8\,\text{m/s}^2$	$U = 0{\cdot}0045\,\text{m/ s}$
$L = 0{\cdot}2980\,\text{m}$	$\varepsilon = 0{\cdot}00003\,^\circ\text{C}^{-1}$	$R = 0{\cdot}0002\,\text{m}^2\,^\circ\text{C/W}$	$V = 0{\cdot}003\omega\cos\omega t\,\text{m/s}$
$S_m^* = 1500\,^\circ\text{C}$	$\rho = 7800\,\text{kg/m}^3$	$m = 10{,}000\,\text{W/m}^2\,^\circ\text{C}$	$\omega = 40(2\pi/60)\,\text{rad/s}$
$T_m^* = 1100\,^\circ\text{C}$	$l = 272\,\text{J/g}$	$\mu = 0{\cdot}5\,\text{Pa}\cdot\text{s}$	$\rho_f = 2930\,\text{kg/m}^3$
$k_s = 1{\cdot}5\,\text{W/m}\,^\circ\text{C}$			

In this example, we consider the case in which liquid remains in the full length of flux channel, *i.e.*, L is taken to be the length of mould wall.

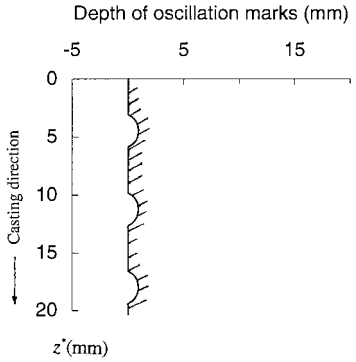

Figure 5. The computed geometry of oscillation marks on steel surface.

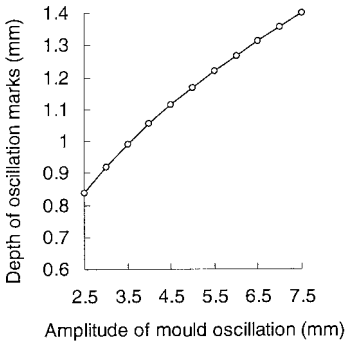

Figure 6. Effect of mould oscillation amplitude on the depth of oscillation marks.

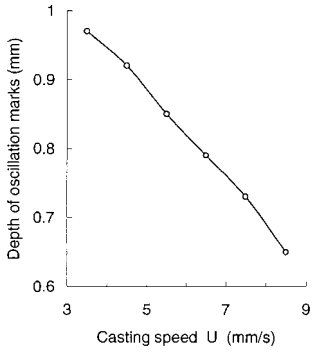

Figure 7. Effect of casting speed U on the depth of oscillation marks.

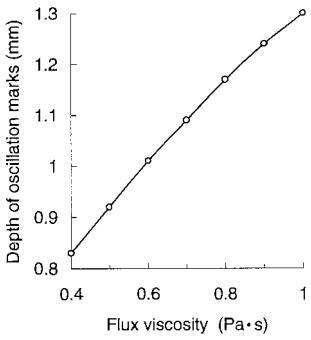

Figure 8. Effect of flux viscosity μ on the depth of oscillation marks.

Figure 5 shows the computed geometry of the oscillation marks on the steel surface. The oscillation marks are regularly spaced with distance about 6·75 mm and depth about 0·9 mm. The prediction of the oscillation mark depth is in the same order of actual depth 0·5 to 2 mm (King *et al.* [8], Please and Dewynne [1], and Cramb and Mannion [12]). Each cycle of mould oscillation includes two distinct stages. In stage one, the gap between the mould wall and the solidified steel shell is open at the solidification point. The gap size varies with time and thus one oscillation mark is produced. In stage two, the gap is closed at the solidification point, which leads to a nearly straight line segment between each two consecutive marks. The shape of the notches appears like hemispherical, which displays certain difference with the actual shape. The actual notches usually are between hemispherical and cusp shaped (Please and Dewynne [1]). The difference between the actual shape and the computed shape probably is caused by our simplifying assumptions such at the stiff beam assumption for the solidified steel shell. To investigate the effect of mould oscillation on the formation of oscillation marks, the amplitude of mould oscillation is varied from 2·5 mm to 7·5 mm and Figure 6 shows the effect of oscillation amplitude on the depth of oscillation marks. The effects of casting speed

and flux viscosity on the geometry of the oscillation marks are respectively shown in Figures 7 and 8. The results indicate that the depth of oscillation marks increases with increasing oscillation amplitude and reducing casting speed, which is in agreement with experiment results at least in qualitative sense.

In conclusion we have extended a previously proposed mechanism for the formation of oscillation marks in the continuous caster which is based on a complete mathematical model, involving coupled heat transfer, solidification and flux flow. The model is illustrated with a numerical example which demonstrates that the appearance of oscillation marks can indeed be predicted by the model and that the depth of marks is critically dependent on the magnitude of the viscosity of the flux, the casting speed and the amplitude of mould oscillation. Although the trends of the model predictions appear to be correct, it should be emphasized that many simplifying assumptions have been made in the development of the model and thus the results should only be used in a qualitative sense. Further work is suggested to construct a more sophisticated model taking into account the latent heat of flux and the elastic-plastic deformation of the solidified steel shell due to the lubrication pressure. However, the new model will be much more complicated and its solution requires intensive numerical work.

List of symbols

A, B	constants involved in (4.4) and Section 7
G, H	functions defined by (4.7)
L	length of liquid flux zone (in z^* direction)
M	the half thickness of cast steel
$P(z^*)$	pressure in liquid flux (assumed independent of x^*)
Q_l	flow rate of liquid flux
Q_s	flow rate of solid flux
Q	$Q_l + Q_s$
Q_R	defined by (3.8)
R	interface thermal contact resistance
S_m^*	melting temperature of steel
$T^*(x^*, z^*, t^*)$	temperature
$T(x, z, t)$	normalized temperature of liquid flux
T_m^*	solidification temperature of liquid mould powder
T_∞^*	temperature of cooling water
T_w^*	temperature on mould wall
T_μ^*	temperature of solid flux on its interface with mould wall
T_0^*	temperature on casting surface
U	casting speed (assumed constant)
$V(t)$	velocity of mould wall
$W(t)$	non-dimensional mould wall velocity (see (5.12))
$X^*(z^*, t^*)$	physical coordinate of the steel phase change boundary
$X(z, t)$	non-dimensional coordinate of the steel phase change boundary
c	specific heat of steel
$f(h), g(h)$	functions defined by (3.10)
g^*	acceleration due to gravity
$h(z^*, t^*)$	thickness of liquid flux layer
$h_0(t^*)$	thickness of liquid flux layer at the solidification point
k	thermal conductivity of steel
k_s	thermal conductivity of solid flux layer
k_t	thermal conductivity of liquid flux layer
l	latent heat of steel
l_f	latent heat of flux
m	surface heat transfer coefficient
p, q	defined by (6.7)
$s(z^*, t^*)$	thickness of solid flux layer
$s_0(t^*)$	thickness of solid flux layer at the solidification point
t^*	time
t_c^*	period of mould oscillation cycle
$u(x^*, z^*)$	flux velocity
z^*	coordinate shown in Figure 3
z_0^*	thickness of the liquid flux layer above the solidification point

α, β, γ	positive constant given by (5.10) and (6.5)
ε	coefficient of linear thermal expansion of steel
η, η_0	defined by (4.8) and (4.10) respectively
λ	positive constant defined by $\varepsilon M/2$
μ	viscosity of liquid flux
Θ	defined by (4.10)
$\theta(z^*, t^*)$	amount of contraction of steel
ρ	density of steel
ρ_f	density of flux
$\Delta\rho$	$\rho - \rho_f$
τ	defined by (6.3)
ω	angular frequency of mould oscillation
ζ	positive parameter used in (3.2), (3.4) and (3.10)
Δz^*	distance between two successive oscillation marks

Note that throughout the superscript * denotes a physical quantity.

Acknowledgment

This research was funded by the Australian Research Council and supported by B.H.P. Newcastle Research Laboratories. The authors are grateful for this support and in particular Dr. Paul Flint of B.H.P. Research who has enthusiastically assisted the program. The authors are particularly grateful to the referees whose comments led to a number of significant improvements.

References

1. C. P. Please and J. N. Dewynne, *Oscillation mark Formation in Continuous Casting.* European Study Group with Industry and Training Course in Mathematical Modeling. Department of Mathematics, University of Southampton, UK (1990) 18pp.
2. E. Takeuchi and J. K. Brimacombe, The formation of oscillation marks in the continuous casting of steel stabs. *Metallurgical Trans.* B15 (1984) 493–509.
3. E. Laitinen and P. Neittaanmaki, On numerical simulation of the continuous casting process. *J. Eng. Math*. 22 (1988) 335–354.
4. M. R. Ridolfi, B. G. Thomas, G. Li and U. Della Foglia, Optimization de la conicité de la lingotière pour la machine de coulée continue de ronds a l'Ilva-Dalmine. *La Revue de Metallurgie – CIT* 91(4) (1994) 609–620.
5. Y. H. Wu and J. M. Hill, A novel finite element method for heat transfer in the continuous caster. *J. Austral. Math. Soc.* B35 (1994) 263–288.
6. D. R. Bland, Flux and the continuous casting of steel. *IMA J. Appl. Math.* 32 (1984) 89–112.
7. N. Fowkes and A. Woods, *The Flux of Flux in a Continuous Steel Caster*. Dep. Math. Preprint, University of Western Australia (1989) 18pp.
8. J. R. King, A. A. Lacey, C. P. Please, P. Wilmott and A. Zoryk, The formation of oscillation marks on continuously cast steel. *Math. Eng. Ind.* 4 (1993) 91–106.
9. N. Fowkes, A. Woods, E. J. Hinch and C. P. Please, Flux consumption in continuous casting. *Oxford Study Group with Industry Report*. Oxford, UK (1988) 1–5.
10. J. M. Hill and Y. H. Wu, On a nonlinear Stefan problem arising in the continuous casting of steel. *Acta Mech.* 107 (1994) 183–198.
11. J. E. Lait, J. K. Brimacombe and F. Weinberg, Mathematical modelling of heat flow in the continuous casting of steel. *Ironmaking and Steelmaking* 1 (1974) 90–97.
12. A. W. Cramb and F. J. Mannion, The measurement of meniscus marks at Bethlehem Steel's Burns Harbor slab caster. In: *Continuous Casting – Interaction between Mould Powders and Other Variables in Continuous Casting*. Iron & Steel Society of AIME, USA (1983) 98–93.